Non linear control Design of the 2-DOF Helicopter (TRMS system)

Samir ZEGHLACHE [(1)], Djamel SAIGAA [(1)], Kamel KARA [(2)]
BOUGUERRA Abderrahmen [(1)]

[(1)] LASS Laboratory, Department of Electronics, Faculty of Technology, University of Msila BP 166 Ichbilia 28000 Algeria

[(2)] Department of Electronics, Faculty of Engineering Sciences, University of Blida, Algeria
zeghlache_samir@yahoo.fr, saigaa_dj@yahoo.fr, k.kara68@gmail.com, rah_bou@yahoo.fr

Abstract- **In this paper, a backstepping controller is designed to position the yaw and pitch angles of a Twin Rotor Multi-input Multi-output System (TRMS). With the coupling effects considered as the uncertainties, the highly coupled nonlinear TRMS is decomposed into a horizontal subsystem and a vertical subsystem. The reaching conditions and the stability of the TRMS with the proposed controller are guaranteed. Finally Simulation results are included to indicate that TRMS with the proposed controller can remain robust to the external disturbances.**

Keywords: TRMS system, Backstepping control, Dynamic model,

I- INTRODUCTION

Helicopters are one of the most manoeuvrable and versatile platforms. They can take-off and landing without a runway and can hover in place. These capabilities have brought about the use of autonomous miniature helicopters. For these reasons, there is currently great interest in using these platforms in a wide range of civil and military applications that include traffic surveillance, search and rescue, air pollution monitoring, area mapping, agriculture applications, bridge and building construction inspection. For performing safely many types of these tasks, high manoeuvrability and robustness of the controllers with respect to disturbances and modelling errors are required. This has generated considerable interest in the robust flight control design. The twin rotor multi-input multi-output system (TRMS) is an aero-dynamical system similar to a helicopter it is characterized by the complicated nonlinearity and the high coupling effect between two propellers [1],[2], many efforts have been made to control the TRMS and some strategies have been developed to solve the path following problems for this type of system. First of this works is in [3] the authors present a comparison of classical control and intelligent control based on fuzzy logic control and genetic algorithm applied to the TRMS system. In [4] presents the evolutionary computation based the genetic algorithm for the parameters optimization of the proportional-integral differential (PID) control to the TRMS system. The goals of control are to stabilize the TRMS in significant cross-couplings. In [5] the design procedures of the fuzzy takagi-sugeno model of TRMS are detailed. Based on the derived fuzzy takagi-sugeno model, parallel distributed fuzzy LQR controller are designed to control the position of the pitch and yaw angles in TRMS.

In [6] a multivariable nonlinear H_∞ controller is designed for the angle control of the TRMS. Since the rotor speeds are assumed to be constant, in [7] investigates the development of an adaptive dynamic nonlinear model inversion control law for a TRMS system utilizing artificial neural networks and genetic algorithms, In [8] a stable neural network based observer for TRMS system is proposed to approximate the nonlinearities of the system. A learning rule for neural network is given which guarantee robustness of the observer. In [9], fuzzy controllers are designed for the tracking of pitch and yaw angles of the TRMS system.

On the other hand, the sliding mode control has been applied extensively to control the non linear system, The advantage of this approach is its insensitivity to the model errors, parametric uncertainties, ability to globally stabilize the system and other disturbances [10], [11]. In [12] a fuzzy sliding and fuzzy integral sliding controller is designed to position the yaw and pitch angles of a TRMS system using the linear surface. To simplify the design of an effective controller for the position control of the pitch and yaw angles, the TRMS is pseudo-decomposed into the horizontal and vertical subsystems. Instead of ignoring the coupling effects between the horizontal and the vertical subsystems, the coupling effects are considered as the uncertainties in the horizontal and the vertical subsystems.

The contribution of our work is used the backstepping control in order to ensuring the locally asymptotic stability and desired tracking trajectories. Unlike to However, Finally all the control laws synthesized are highlighted by simulations which gave results considered to be satisfactory.

The remainder of this paper is organized as follows. The dynamics of the TRMS is described in Section II. In Section III, the decomposed model of the TRMS is introduced. Section IV present the backstepping designed and simulation results to demonstrate the effectiveness of our approach. Finally we arrive to the conclusion of the whole work in section V.

II- MODEL DESCRIPTION OF THE TRMS

Similar to most flight vehicles, the helicopter consists of several elastic parts such as rotor, engine and control surfaces. The nonlinear aerodynamic forces and gravity act on

the vehicle, and flexible structures increase complexity and make a realistic analysis difficult. For control purpose, it is necessary to find a representative model that shows the same dynamic characteristics as the real aircraft [8]. The behaviour of a nonlinear TRMS, (shown in Fig. 1), in certain aspects resembles that of a helicopter. It can be well perceived as a static test rig for an air vehicle with formidable control challenges.

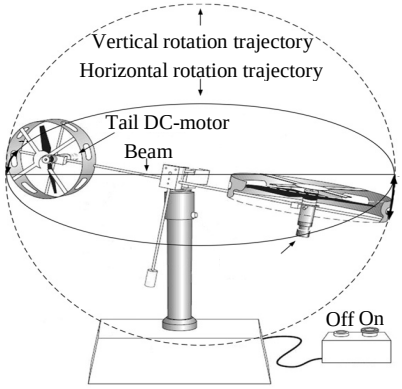

Fig.1. The twin rotor multi-input multi-output system (TRMS) [13]

This TRMS consists of a beam pivoted on its base in such a way that it can rotate freely in both its horizontal and vertical planes. There are two rotors (the main and tail rotors), driven by DC motors, at each end of the beam. If necessary, either or both axes of rotation can be locked by means of two locking screws provided for physically restricting the horizontal or vertical plane rotation. Thus, the system permits both 1 and 2 degree-of-freedom (DOF) experiments. The two rotors are controlled by variable speed electric motors enabling the helicopter to rotate in a vertical and horizontal plane (pitch and yaw). The tail rotor could be rotated in either direction, allowing the helicopter to yaw right or left. The motion of the helicopter was damped by a pendulum, which hung from a central pivot point. In a typical helicopter, the aerodynamic force is controlled by changing the angle of attack of the blades. The laboratory setup is constructed such that the angle of attack of the blades is fixed. The aerodynamic force is controlled by varying the speed of the motors. The mathematical model of the TRMS is developed under following assumptions.

- The dynamics of the propeller subsystem can be described by first-order differential equations.
- The friction in the system is of the viscous type.
- The propeller – air subsystem could be described in accordance with the postulates of the flow theory.

The mechanical system of TRMS is simplified using a four point-mass system shown in Fig. 2, includes main rotor, tail rotor, balance-weight and counter-weight. Based on Lagrange's equations, we can classify the mechanical system into two parts, the forces around the horizontal axis and the forces around the vertical axis.

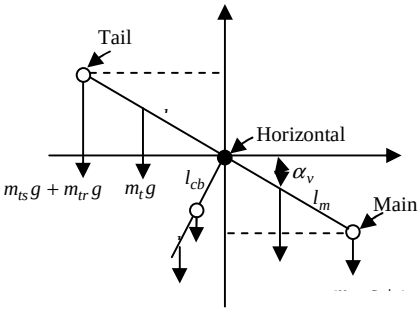

Fig.2. Simplified four point-mass system [13]

The parameters in the simplified four point-mass system are M_{v1} is the return torque corresponding to the force of gravity, M_{v2} is the moment of a aerodynamic force, M_{v3} is the moment of a centrifugal forces, M_{v4} is a Moment of friction, m_{mr} is the mass of the DC motor within the main rotor, m_m is the mass of the main part of the beam, m_{tr} is the mass of the DC motor within tail rotor, m_t is the mass of the tail part of the beam, m_{cb} is the mass of the counter weight, m_b is the mass of the counter-weight beam, m_{ms} is the mass of the main shield, m_{ts} is the mass of the tail shield, l_m is the length of the main part of the beam, l_t is the length of the tail part of the beam, l_b is the length of the counter-weight beam, l_{cb} is the distance between the counter-weight and joint, and g is the gravitational acceleration.

Consider the rotation of the beam in the vertical plane (around the horizontal axis). The driving torqueses are produced by the propellers, and the rotation can be described in principle as the motion of a pendulum. We can write the equations describing this motion as follows.

a) The main rotor model

$$M_{v1} = g\left\{\left[\left(\frac{m_t}{2} + m_{tr} + m_{ts}\right)l_t - \left(\frac{m_m}{2} + m_{mr} + m_{ms}\right)l_m\right]\cos\alpha_v - \left(\frac{m_b}{2}l_b + m_{cb}\ l_{cb}\right)\sin\alpha_v\right\} \quad (1)$$

$$M_{v1} = g\left\{[A - B]\cos\alpha_v - C\sin\alpha_v\right\} \quad (2)$$

With:

$$\begin{cases} A = \left(\frac{m_t}{2} + m_{tr} + m_{ts}\right)l_t \\ B = \left(\frac{m_m}{2} + m_{mr} + m_{ms}\right)l_m \\ C = \left(\frac{m_b}{2}l_b + m_{cb}\ l_{cb}\right) \end{cases} \quad (3)$$

$$M_{v2} = l_m S_f F_v(\omega_m) \quad (4)$$

The angular velocity ω_m of main propeller is a nonlinear function of a rotation angle of the DC motor describing by:

$$\omega_m(u_{vv}) = 90.90\,u_{vv}^6 + 599.73\,u_{vv}^5 - 129.26\,u_{vv}^4 - 1238.64\,u_{vv}^3 + 63.45\,u_{vv}^2 + 1238.41\,u_{vv} \quad (5)$$

Also, the propulsive force F_v moving the joined beam in the vertical direction is describing by a nonlinear function of the angular velocity ω_m

$$F_v(\omega_m) = -3.48\times10^{-12}\omega_m^5 + 1.09\times10^{-9}\omega_m^4 + 4.123\times10^{-6}\omega_m^3 - 1.632\times10^{-4}\omega_m^2 + 9.544\times10^{-2}\omega_m \quad (6)$$

The model of the motor-propeller dynamics is obtained by substituting the nonlinear system by a serial connection of a linear dynamics system. This can be expressed as:

$$\frac{du_{vv}}{dt} = \frac{1}{T_{mr}}(-u_{vv} + u_v) \quad (7)$$

u_v is the input voltage of the DC motor, T_{mr} is the time constant of the main rotor and K_{mr} is the static gain DC motor.

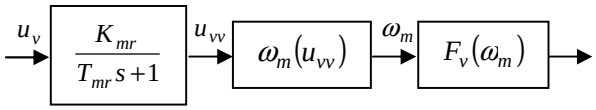

Fig 3. The relationship between the input voltage and the propulsive force for the main rotor [13]

$$M_{v3} = -\Omega_h^2\left\{\left(\frac{m_t}{4}+m_{tr}+m_{ts}\right)l_t^2 + \left(\frac{m_t}{4}+m_{tr}+m_{ts}\right)l_m^2 - \left(\frac{m_b}{4}l_b^2 + m_{tb}l_{cb}^2\right)\right\}\sin\alpha_v\cos\alpha_v \quad (8)$$

$$M_{v3} = -\Omega_h^2(H)\sin\alpha_v\cos\alpha_v \quad (9)$$

With:

$$H = \left(\frac{m_t}{4}+m_{tr}+m_{ts}\right)l_t^2 + \left(\frac{m_t}{4}+m_{tr}+m_{ts}\right)l_m^2 - \left(\frac{m_b}{4}l_b^2 + m_{tb}l_{cb}^2\right) \quad (10)$$

$$\Omega_h = \frac{d\alpha_h}{dt} \quad (11)$$

$$M_{v4} = -\Omega_v K_v \quad (12)$$

$$\Omega_v = \frac{d\alpha_v}{dt} \quad (13)$$

$$\frac{dS_v}{dt} = \frac{1}{J_v}\sum_{i=1}^{4} M_{vi} \quad (14)$$

$$\frac{dS_v}{dt} = \frac{1}{J_v}\{l_m S_f F_v(\omega_m) - K_v\Omega_v + g((A-B)\cos\alpha_v - C\sin\alpha_v) - \Omega_h^2(H)\sin\alpha_v\cos\alpha_v\} \quad (15)$$

$$\frac{d\alpha_v}{dt} = \Omega_v = S_v + \frac{J_{tr}\omega_t}{J_v} \quad (16)$$

Where ω_t is the angular velocity of tail propeller, S_v the angular momentum in the vertical plane of the beam, J_v the sum of inertia moments in the horizontal plane, J_{tr} the moment of inertia in DC motor tail propeller subsystem, K_v the Friction constant, and S_f the balance scale.

b) The tail rotor model

Similarly, we can describe the motion of the beam in the horizontal plane (around the vertical axis) as shown in Fig.4. The driving torqueses are produces by the rotors and that the moment of inertia depends on the pitch angle of the beam.

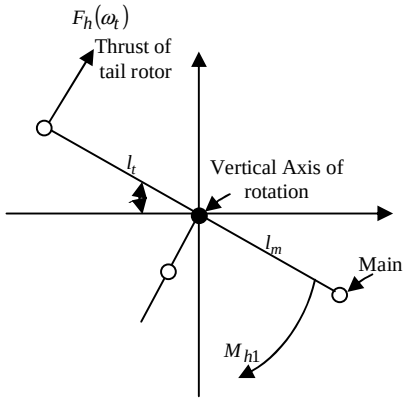

Fig 4. Torques around the vertical axis [13]

The parameters in the torques around vertical axis are M_{h1} is the moment of a aerodynamic force, M_{h2} is a Moment of friction.

$$M_{h1} = l_t S_f F_h(\omega_t)\cos\alpha_v \quad (17)$$

The angular velocity ω_t of tail propeller is a nonlinear function of a rotation angle of the DC motor describing by:

$$\omega_t(u_{hh}) = 2020\,u_{hh}^5 + 194.69\,u_{hh}^4 - 4283.15\,u_{vv}^3 - 262.87\,u_{hh}^2 + 3796.83\,u_{hh} \quad (18)$$

Also, the propulsive force F_h moving the joined beam in the Horizontal direction is describing by a nonlinear function of the angular velocity ω_t

$$F_h(\omega_t) = -3\times10^{-14}\omega_t^5 + 1.595\times10^{-11}\omega_t^4 + 2.511\times10^{-7}\omega_t^3 - 1.808\times10^{-4}\omega_t^2 + 0.8080\ \omega_t \quad (19)$$

The model of the motor-propeller dynamics is obtained by substituting the nonlinear system by a serial connection of a linear dynamics system. This can be expressed as:

$$\frac{du_{hh}}{dt} = \frac{1}{T_{tr}}(-u_{hh} + u_h) \quad (20)$$

u_h is the input voltage of the DC motor, T_{tr} is the time constant of the tail rotor and K_{tr} is the static gain DC motor .

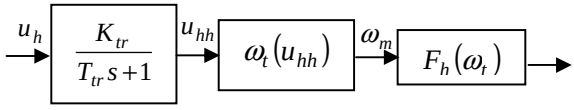

Fig 5. The relationship between the input voltage and the propulsive force for the tail rotor [13]

$$M_{h2} = -\Omega_h K_h \tag{21}$$

$$\frac{dS_h}{dt} = \frac{1}{J_h(\alpha_v)} \sum_{i=1}^{4} M_{hi} \tag{22}$$

$$J_h(\alpha_v) = D\cos^2\alpha_v + E\sin^2\alpha_v + F$$

$$\frac{dS_h}{dt} = \frac{l_t S_f F_h(\omega_t)\cos\alpha_v - \Omega_h K_h}{J_h(\alpha_v)} \tag{23}$$

$$\frac{dS_h}{dt} = \frac{l_t S_f F_h(\omega_t)\cos\alpha_v - \Omega_h K_h}{D\cos^2\alpha_v + E\sin^2\alpha_v + F} \tag{24}$$

$$\frac{d\alpha_h}{dt} = \Omega_h = S_h + \frac{J_{mr}\,\omega_m\cos\alpha_v}{D\cos^2\alpha_v + E\sin^2\alpha_v + F} \tag{25}$$

Where S_h the angular momentum in the horizontal plane of the beam, J_h the sum of inertia moments in the vertical plane, J_{mr} the moment of inertia in DC motor main propeller subsystem, K_h the Friction constant, and S_f the balance scale.

The dynamics of the TRMS system are described as follows

$$\begin{cases} \dfrac{dS_v}{dt} = \dfrac{1}{J_v}\{\, l_m S_f F_v(\omega_m) - K_v\Omega_v + g((A-B)\cos\alpha_v - C\sin\alpha_v) \\ \qquad -\Omega_h^2(H)\sin\alpha_v\cos\alpha_v \,\} \\ \Omega_v = \dfrac{d\alpha_v}{dt} \\ \Omega_v = S_v + \dfrac{J_{tr}\omega_t}{J_v} \\ \dfrac{dS_h}{dt} = \dfrac{l_t S_f F_h(\omega_t)\cos\alpha_v - \Omega_h K_h}{J_h(\alpha_v)} \\ \Omega_h = \dfrac{d\alpha_h}{dt} \\ \Omega_h = S_h + \dfrac{J_{mr}\omega_m\cos\alpha_v}{D\cos^2\alpha_v + E\sin^2\alpha_v + F} \end{cases} \tag{26}$$

The model developed in (26) can be rewritten in the state-space form:

$\dot{X} = f(x) + g(X,U)$ and $X = [x_1,...,x_6]^T$ is the state vector of the system such as:

$$X = [\alpha_v, S_v, u_{vv}, \alpha_h, S_h, u_{hh}] \tag{27}$$

$$U = [u_v, u_h] \tag{28}$$

$$\mathrm{Y} = [\alpha_v, \alpha_h] \tag{29}$$

From (26), (28) and (29) we obtain the following state representation:

$$\begin{cases} \dot{x}_1 = x_2 + \dfrac{J_{tr}}{J_v}\omega_t(x_6) \\ \dot{x}_2 = \dfrac{1}{J_v}\left\{ \begin{array}{l} l_m S_f F_v(\omega_m(x_3)) - K_v\left(x_2 + \dfrac{J_{tr}}{J_v}\omega_t(x_6)\right) + g((A-B)\cos x_1 - C\sin x_1) \\ \quad -\left(x_5 + \dfrac{J_{mr}\omega_m(x_3)\cos x_1}{D\cos^2 x_1 + E\sin^2 x_1 + F}\right)^2 (H)\sin x_1\cos x_1 \end{array} \right\} \\ \dot{x}_3 = \dfrac{1}{T_{mr}}(-x_3 + K_{mr}u_v) \\ \dot{x}_4 = x_5 + \dfrac{J_{mr}\omega_m(x_3)\cos x_1}{D\cos^2 x_1 + E\sin^2 x_1 + F} \\ \dot{x}_5 = \dfrac{1}{D\cos^2 x_1 + E\sin^2 x_1 + F}\left\{ l_t S_f F_h(\omega_t)\cos\alpha_v - K_h\left(x_5 + \dfrac{J_{mr}\omega_m(x_3)\cos x_1}{D\cos^2 x_1 + E\sin^2 x_1 + F}\right)\right\} \\ \dot{x}_6 = \dfrac{1}{T_{tr}}(-x_6 + K_{tr}u_h) \end{cases} \tag{30}$$

III. DECOUPLED MODELS OF THE TRMS SYSTEM

Since the characteristic of TRMS is very complex in the nature, it would be convenient to design a controller for TRMS with the TRMS decoupled into horizontal and vertical subsystems by fixing the horizontal angle α_h and posing $u_h = 0$, from Eq. (30), it is easy to see that state equations with the state vector X_v for the vertical subsystem of the TRMS could be defined as:

$$X_v = [x_1, x_2, x_3] = [\alpha_v, S_v, u_{vv}] \tag{31}$$

$$\begin{cases} \dot{x}_1 = x_2 \\ \dot{x}_2 = \dfrac{1}{J_v}\{l_m S_f F_v(\omega_m(x_3)) - K_v(x_2) + g((A-B)\cos x_1 - C\sin x_1)\} \\ \dot{x}_3 = \dfrac{1}{T_{mr}}(-x_3 + K_{mr}u_v) \end{cases} \tag{32}$$

Where u_v is a control action of the vertical subsystem Likewise, we have the horizontal subsystem by posing $\alpha_v = \alpha_v(0) = \alpha_{v0}$ and $u_v = 0$

$$X_v = [x_1, x_2, x_3] = [\alpha_v, S_v, u_{vv}] \tag{33}$$

$$\begin{cases} \dot{x}_4 = x_5 \\ \dot{x}_5 = \dfrac{1}{J_h(\alpha_{v0})}\{l_t S_f F_h(\omega_t)\cos\alpha_{v0} - K_h x_5\} \\ \dot{x}_6 = \dfrac{1}{T_{tr}}(-x_6 + K_{tr}u_h) \end{cases} \tag{34}$$

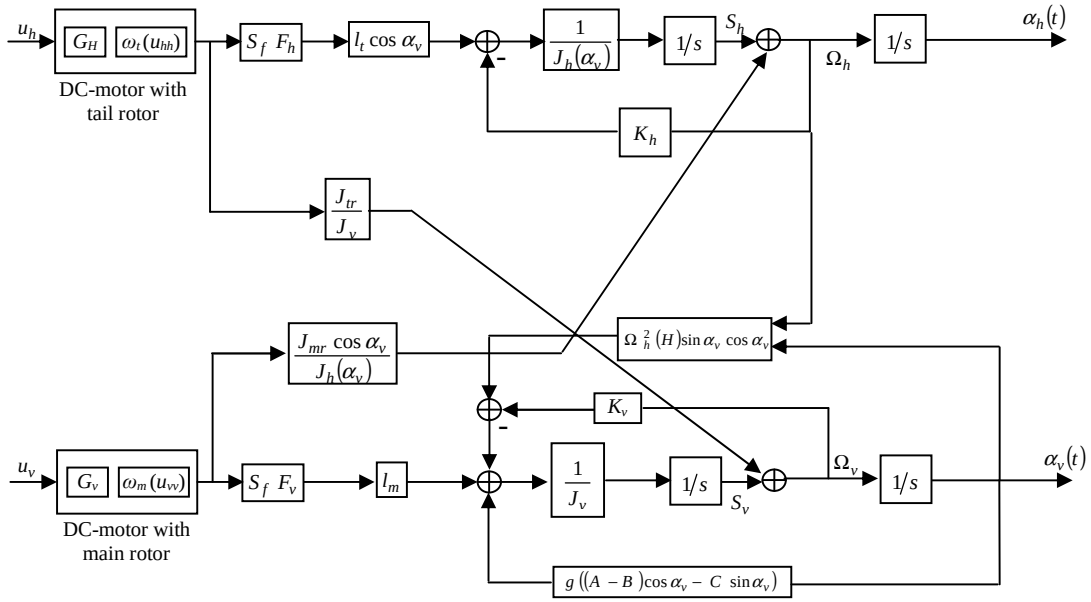

Fig.6. Block diagram of TRMS system [13]

IV. BACKSTEPPING CONTROLLER DESIGN

The backstepping approach as a recursive algorithm for the control-low synthesis, we all the stages of calculation concerning the tracking errors and lyapunov function. From (32) we obtain the following state representation of the vertical subsystem

$$\begin{cases} \dot{x}_1 = x_2 \\ \dot{x}_2 = f_v(x_3) - b_v x_2 + g_v(x_1) \\ \dot{x}_3 = -C_v x_3 + d_v u_v \end{cases} \tag{35}$$

$$\begin{cases} b_v = \dfrac{K_v}{J_v} \\ c_v = \dfrac{1}{T_{mr}},\ d_v = \dfrac{K_{mr}}{T_{mr}} \end{cases} \tag{36}$$

$$\begin{cases} f_v(x_3) = \dfrac{l_m}{J_v} S_f F_v(\omega_m(x_3)) \\ g_v(x_1) = \dfrac{g}{J_v}((A-B)\cos(x_1) - C\sin(x_1)) \end{cases} \tag{37}$$

The first error considered in designing the backstepping

$$z_{1v} = x_1 - x_{1d} = \alpha_v - \alpha_{vd}$$

Lyapunov theory is used while using the Lyapunov function z_{1v} as a positive definite and its time derivative as a negative semi definite,

$$V_{1v} = \frac{1}{2} z_{1v}^2$$

Its derivative is given by

$$V_{1v} = z_{1v}\dot{z}_{1v} = z_{1v}(x_2 - \dot{x}_{1d}) \tag{38}$$

There is no control input in (38). By letting x_2 be the virtual control, the desired virtual control is defined as:

$$(x_2)_d = -\alpha_{1v} z_{1v} + \dot{x}_{1d} \qquad \alpha_{1v} > 0$$

Where α_{1v} is a positive constant for increasing the convergence speed of the vertical angle tracking loop.

Now, the virtual control is x_2 where the second error tracking is defined by:

$$z_{2v} = x_2 - (x_2)_d = x_2 + \alpha_{1v} z_{1v} - \dot{x}_{1d}$$

The augmented Lyapunov function for the second step is given by

$$V_{2v} = \frac{1}{2} z_{1v}^2 + \frac{1}{2} z_{2v}^2 \tag{39}$$

The derivative of (53) is given by:

$$\dot{V}_{2v} = z_{1v}\dot{z}_{1v} + z_{2v}\dot{z}_{2v} \tag{40}$$

By putting $\dot{z}_{2v}$ in (40), the following can be obtained

$$\dot{V}_{2v} = z_{1v}\dot{z}_{1v} + z_{2v}\left(f_v(x_3) - b_v x_2 + g_v(x_1) - \alpha_{v1}\left(x_2 - \dot{x}_{1d}\right) - \ddot{x}_{1d}\right) \tag{41}$$

By letting $f_v(x_3) + g_v(x_1)$ be the virtual control, the desired virtual control in the second step is defined as:

$$(f_v(x_3) + g_v(x_1))_d = -\alpha_{v2} z_{2v} + b_v x_2 + \alpha_{v1}(x_2 - \dot{x}_{1d}) - \ddot{x}_{1d} \tag{42}$$

Now, the virtual control is $f_v(x_3) + g_v(x_1)$ where the sliding surface is defined in the third step by:

$$z_{3v} = f_v(x_3) + g_v(x_1) - (f_v(x_3) + g_v(x_1))_d \tag{43}$$

$$= f_v(x_3) + g_v(x_1) + \alpha_{v2} z_{2v} - \ddot{x}_{1d} - \alpha_{v1}(x_2 - \dot{x}_{1d}) - b_v x_2 \tag{44}$$

The augmented Lyapunov function for the third step is given by

$$V_{3v} = \frac{1}{2} z_{1v}^2 + \frac{1}{2} z_{2v}^2 + \frac{1}{2} z_{3v}{}^2 \quad (45)$$

The derivative of (45) is given by:

$$\dot{V}_{3v} = z_{1v}\dot{z}_{1v} + z_{2v}\dot{z}_{2v} + z_{3v}\dot{z}_{3v} \quad (46)$$

By putting $\dot{z}_{3v}$ in (46), the following can be obtained

$$\dot{V}_{3v} = z_{1v}\dot{z}_{1v} + z_{2v}\dot{z}_{2v} + z_{3v}\begin{pmatrix} \frac{\partial f_v(x_3)}{\partial x_3}\dot{x}_3 + \frac{\partial g_v(x_1)}{\partial x_1} + \alpha_{v2}\left(\dot{x}_2 + \alpha_{v1}\left(x_2 - \dot{x}_{1d}\right) - \ddot{x}_{1d}\right) \\ -\ddot{x}_{1d} - \alpha_{v1}\left(\dot{x}_2 - \ddot{x}_{1d}\right) - b_v\dot{x}_2 \end{pmatrix} \quad (47)$$

As for the backstepping approach, the control input u_v is extracted:

$$u_v = \frac{1}{d_v \frac{\partial f_v(x_3)}{\partial x_3}} \begin{bmatrix} c_v \frac{\partial f_v(x_3)}{\partial x_3} x_3 + \alpha_{v2}\left(\dot{x}_2 + \alpha_{v1}\left(x_2 - \dot{x}_{1d}\right) - \ddot{x}_{1d}\right) + \dddot{x}_{1d} + \\ b_v\left(f_v(x_3) - b_v x_2 + g_v(x_1)\right) - \frac{\partial g_v(x_1)}{\partial x_1} x_2 - \alpha_{v3} z_{3v} \\ -\alpha_{v2}\dot{z}_{2v} + \alpha_{v1}\ddot{z}_{1v} \end{bmatrix} \quad (48)$$

Likewise From (34) we obtain the following state representation of the horizontal subsystem

$$\begin{cases} \dot{x}_4 = x_5 \\ \dot{x}_5 = f_h(x_6) - b_h x_5 \\ \dot{x}_6 = -C_h x_6 + d_h u_h \end{cases} \quad (49)$$

$$\begin{cases} b_h = \dfrac{K_h}{J_h(\alpha_{v0})} \\ c_h = \dfrac{1}{T_{tr}},\ d_h = \dfrac{K_{tr}}{T_{tr}} \\ f_h(x_6) = \dfrac{l_t}{J_h(\alpha_{v0})} S_f F_h(\omega_t(x_6))\cos(\alpha_{v0}) \end{cases} \quad (50)$$

The first error considered in designing the backstepping

$$z_{1h} = x_4 - x_{4d} = \alpha_h - \alpha_{hd}$$

Lyapunov theory is used while using the Lyapunov function z_{1h} as a positive definite and its time derivative as a negative semi definite,

$$V_{1h} = \frac{1}{2} z_{1h}^2$$

Its derivative is given by

$$\dot{V}_{1h} = z_{1h}\dot{z}_{1h} = z_{1h}\left(x_5 - \dot{x}_{4d}\right) \quad (51)$$

There is no control input in (50). By letting x_5 be the virtual control, the desired virtual control is defined as:

$$(x_5)_d = -\alpha_{h1} z_{1h} + \dot{x}_{4d} \qquad \alpha_{1h} > 0 \quad (52)$$

Where α_{h1} is a positive constant for increasing the convergence speed of the vertical angle tracking loop.

Now, the virtual control is x_5 where the second error tracking is defined by:

$$z_{2h} = x_5 - (x_5)_d = x_5 + \alpha_{h1} z_{1h} - \dot{x}_{4d}$$

The augmented Lyapunov function for the second step is given by

$$V_{2h} = \frac{1}{2} z_{1h}^2 + \frac{1}{2} z_{2h}^2 \quad (53)$$

The derivative of (53) is given by:

$$\dot{V}_{2h} = z_{1h}\dot{z}_{1h} + z_{2h}\dot{z}_{2h} \quad (54)$$

By putting $\dot{z}_{2h}$ in (54), the following can be obtained

$$\dot{V}_{2h} = z_{1h}\dot{z}_{1h} + z_{2h}\left(f_h(x_6) - b_h x_5 - \alpha_{h1}\left(x_4 - \dot{x}_{4d}\right) - \ddot{x}_{4d}\right) \quad (55)$$

By letting $f_h(x_6)$ be the virtual control, the desired virtual control in the second step is defined as:

$$(f_h(x_6))_d = -\alpha_{h2} z_{2v} + b_h x_5 + \alpha_{h1}\left(x_4 - x_{4d}\right) - \ddot{x}_{4d} \quad (56)$$

Now, the virtual control is $f_h(x_6)$ where the sliding surface is defined in the third step by:

$$z_{3h} = S_h = f_h(x_6) - (f_h(x_6))_d \quad (57)$$

$$= f_h(x_6) + \alpha_{h2} z_{2h} - \ddot{x}_{4d} - \alpha_{h1}\left(x_5 - \dot{x}_{4d}\right) - b_h x_5 \quad (58)$$

The augmented Lyapunov function for the third step is given by:

$$V_{3h} = \frac{1}{2} z_{1h}^2 + \frac{1}{2} z_{2h}^2 + \frac{1}{2} z_{3h}^2 \quad (59)$$

The derivative of (59) is given by:

$$\dot{V}_{3h} = z_{1h}\dot{z}_{1h} + z_{2h}\dot{z}_{2h} + z_{3h}\dot{z}_{3h} \quad (60)$$

By putting $\dot{z}_{3h}$ in (60), the following can be obtained

$$\dot{V}_{3h} = z_{1h}\dot{z}_{1h} + z_{2h}\dot{z}_{2h} + z_{3h}\begin{pmatrix} \frac{\partial f_h(x_6)}{\partial x_6}\dot{x}_6 + \alpha_{h2}\left(\dot{x}_5 + \alpha_{h1}\left(x_5 - \dot{x}_{4d}\right) - \ddot{x}_{4d}\right) \\ -\dddot{x}_{4d} - \alpha_{h1}\left(\dot{x}_5 - \ddot{x}_{4d}\right) - b_h\dot{x}_5 \end{pmatrix} \quad (61)$$

As for the backstepping approach, the control input u_h is extracted:

$$u_h = \frac{1}{d_h \frac{\partial f_h(x_6)}{\partial x_6}} \begin{bmatrix} c_h \frac{\partial f_v(x_6)}{\partial x_6} x_6 + \alpha_{h2}\left(\dot{x}_5 + \alpha_{h1}\left(x_5 - \dot{x}_{4d}\right) - \ddot{x}_{4d}\right) + \dddot{x}_{4d} \\ +b_h\left(f_h(x_6) - b_h x_5\right) - \alpha_{3h}\dddot{z}_{3h} - \alpha_{2h}\ddot{z}_{2h} + \alpha_{1h}\dot{z}_{1h} \end{bmatrix} \quad (65)$$

V. SIMULATION RESULTS

To show the performance of the proposed approach, the corresponding algorithm is implemented in simulation to the TRMS model as shown in fig.6. The results obtained for the vertical and horizontal subsystems are given in the Fig.7, and Fig.8. One can see that, the backstepping controller ensures a good tracking. To show the robustness of the TRMS with the backstepping controller, an external disturbance is added to each of the vertical and horizontal angle at *t=10 sec*. From the performance of the TRMS in Fig.9, it can be seen that the TRMS with the backstepping controller is robust to the external disturbances.

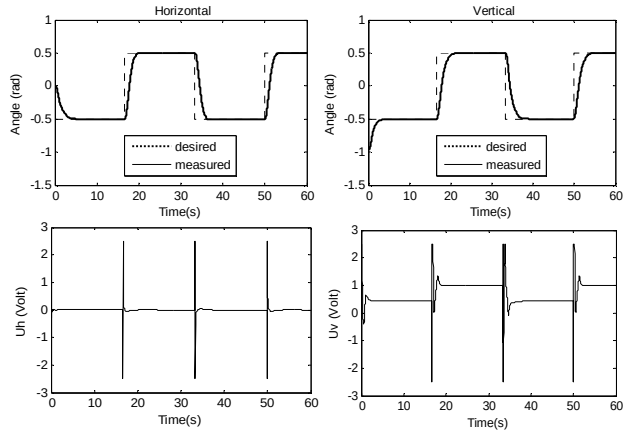

Fig.7. square wave responses of the TRMS with Backstepping control

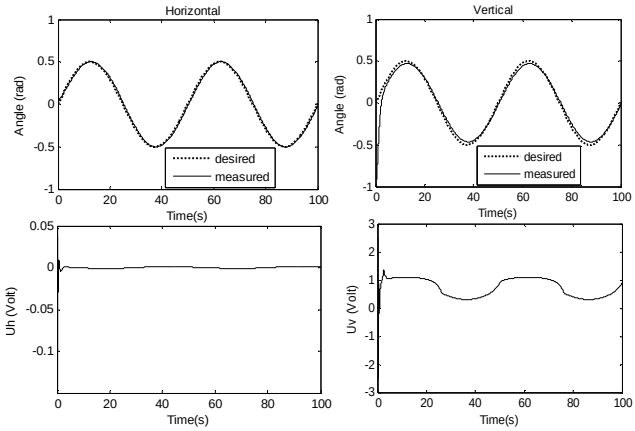

Fig.8. Sine wave responses of the TRMS with Backstepping control

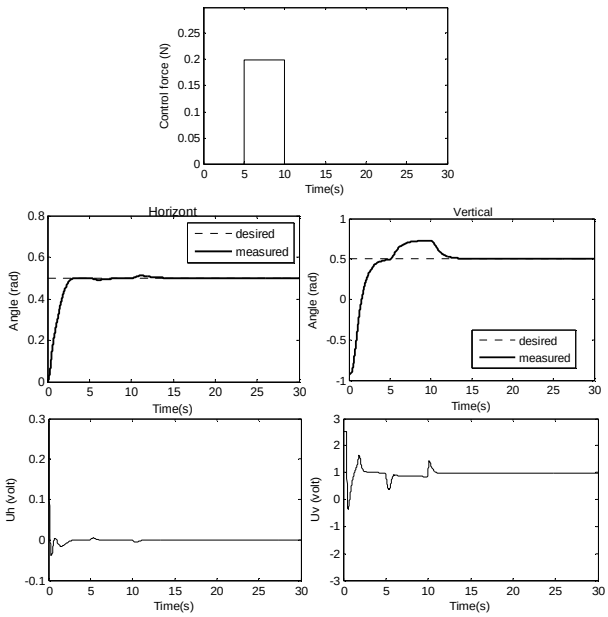

Fig.9. Step responses of the TRMS with the backstepping subject to the external disturbance

VI. CONCLUSION

In this paper, we presented stabilizing control laws synthesis by backstepping technique. Firstly, we start by the development of the dynamic model of the TRMS taking into account the different physics phenomena. A highly coupled nonlinear TRMS is decomposed into a set of horizontal and vertical subsystems with the coupling effect considered as the uncertainties. Simulation results also validate that the presented backstepping has a satisfactory tracking performance.

REFERENCES

[1] K. P. Tee, S. S. Ge, and F. E. H. Tay, "Adaptive neural network control for helicopters in vertical flight," *IEEE Trans. on Control Systems Technology*, vol. 16, no. 4, pp. 753-762, 2008.

[2] P. Wen and T.W. Lu, "Decoupling Control of a twin rotor MIMO system using robust deadbeat control technique," IET Control Theory and Applications, vol. 2, no. 11, pp. 999-1007, 2008.

[3] J. G. Juang, R. W. Lin, and W. K. Liu, "Comparison of classical control and intelligent control for a MIMO cystem," Applied Mathematics and Computation, vol. 205, no. 2, pp. 778-791, 2008.

[4] J. G. Juang, M. T. Huang, and W. K. Liu, "PID control using researched genetic algorithms for a MIMO system," *IEEE Trans. on Systems, Man and Cybernetics: Part C*, vol. 38, no. 5, pp.716-727, 2008.

[5] C.W.Tao, J.S.Taurb and Y.C.Chen," Design of a parallel distributed fuzzy LQR controller for the twin rotor multi-input multi-output system," Fuzzy Sets and Systems, vol. 161, no. 1, pp. 2081–2103, 2010.

[6] M. López-Martinez, C. Vivas, and M.G. Ortega, "A multivariable nonlinear H∞ controller for a laboratory helicopter," IEEE Conf. on European Control, pp. 4065-4070, 2005.

[7] A.Rahideh, M.H.Shaheed, and A.H. Bajodah," Adaptive Nonlinear Model Inversion Control of a Twin Rotor System Using Artificial Intelligence, " IEEE Conf on Control Applications, pp. 898-903, 2007.

[8] F.A.Shaik and S.Purwar," A Nonlinear State Observer Design for 2 – DOF Twin Rotor System Using Neural Networks, " IEEE Conf on Advances in Computing, Control, and Telecommunication Technologies, pp. 15-19, 2009.

[9] C. S. Liu, and al., "Improvement of the twin rotor MIMO system tracking and transient response using fuzzy control technology,'' IEEE Congress on Industrial Electronics and Applications, pp. 1-6, 2006.

[10] V. Utkin, "Variable structure systems with sliding modes" *IEEE Trans. On Automatic Control*, vol. 22, no. 2, pp. 212-222, 1977.

[11] J. Y. Hung, W. Gao and J. C. Hung, "Variable structure control: a survey," *IEEE Trans on Industrial Electronics*, vol. 40, no. 1, pp. 2-22, 1993.

[12] C.W Tao, J.S. Taur, Y.H.Chang, C.W.Chang," A Novel Fuzzy Sliding and Fuzzy Integral Sliding Controller for the Twin Rotor Multi-Input Multi-Output System," IEEE Trans. on Fuzzy Systems, vol. 18, no. 4, pp. 1-12, 2010.

[13] Feedback Instruments Ltd., Twin Rotor MIMO System Advanced Technique Manual 33-007-4M5, E. Sussex, England, 1997.